

Thermodynamics of the interaction of xanthine oxidase with superoxide dismutase studied by isothermal titration calorimetry and fluorescence spectroscopy

Yu-Ling Zhou, Jun-Ming Liao, Fen Du, Yi Liang*

Key Laboratory of MOE for Virology, College of Life Sciences, Wuhan University, Wuhan 430072, China

Received 17 April 2004; received in revised form 9 July 2004; accepted 29 July 2004

Available online 28 August 2004

Abstract

Xanthine oxidase (XO) and copper, zinc superoxide dismutase (Cu, Zn-SOD) are function-related proteins in vivo. Thermodynamics of the interaction of bovine milk XO with bovine erythrocyte Cu, Zn-SOD has been studied using isothermal titration calorimetry (ITC) and fluorescence spectroscopy. The binding of XO to Cu, Zn-SOD is driven by a large favorable enthalpy decrease with a large unfavorable entropy reduction, and shows strong entropy–enthalpy compensation and weak temperature-dependence of Gibbs free energy change. An unexpected, large positive molar heat capacity change of the binding, $3.02 \text{ kJ mol}^{-1} \text{ K}^{-1}$, at all temperatures examined suggests that either hydrogen bond or long-range electrostatic interaction is a major force for the binding. XO quenches the intrinsic fluorescence of Cu, Zn-SOD and causes a small red shift in the fluorescence emission maximum of the protein. A small salt concentration dependence of the binding affinity measured by fluorescence spectroscopy and a large unfavorable change in entropy for the binding measured by ITC suggest that long-range electrostatic forces do not play an important role in the binding. These results indicate that XO binds to Cu, Zn-SOD with high affinity and that hydrogen bond is a major force for the binding.

© 2004 Elsevier B.V. All rights reserved.

Keywords: Isothermal titration calorimetry; Protein–protein interactions; Superoxide dismutase; Thermodynamics; Xanthine oxidase

1. Introduction

Protein–protein interactions (PPIs) play key roles in many essential biological processes such as the assembly of cellular components, the transport machinery across the various biological membranes, signal transduction, and the regulation of gene expression and enzymatic activities [1–4]. Aberrant or perturbed PPIs have been implicated in a number of diseases such as Alzheimer's disease and cancer [3].

Isothermal titration calorimetry (ITC) is an important tool for the study of both thermodynamic and kinetic properties of biological macromolecules by virtue of its general applicability and high precision, as shown by recent developments

[1,5–10]. This method has yielded a large amount of useful thermodynamic data on PPIs [1,5,6,9–18].

Xanthine oxidase (XO, EC 1.2.3.2), a very important enzyme in the purine metabolism, is a 290 kDa homodimer possessing two iron-sulfur centers and one flavin adenine dinucleotide (FAD) in addition to one molybdenum center in each of the subunits [19,20]. It catalyzes the oxidation of hypoxanthine to xanthine and of xanthine to uric acid, producing two reactive oxygen species (ROS), superoxide anion radical ($\text{O}_2^{\bullet-}$) and hydrogen peroxide (H_2O_2) [21–23]. Higher amounts of ROS are thought to underlie the pathogenesis of various diseases, including cancer and influenza virus infection [23,24]. Whereas copper, zinc superoxide dismutase (Cu, Zn-SOD, EC 1.15.1.1), a 32 kDa homodimer containing two copper and two zinc ions per dimer [25]. It catalyzes the dismutation of $\text{O}_2^{\bullet-}$ to H_2O_2 and molecular oxygen by alternately oxidizing and reducing the copper [26–28], and has

* Corresponding author. Tel.: +86 27 8721 4902; fax: +86 27 8766 9560.
E-mail address: liangyi@whu.edu.cn (Y. Liang).

great physiological significance and therapeutic potential for diseases associated with ROS [23,24,29]. Because XO and Cu, Zn-SOD are function-related proteins in vivo [23,30], it is of interest to determine whether XO binds to Cu, Zn-SOD with high affinity. The purpose of this investigation is to provide detailed thermodynamic and kinetic data for the interaction of XO with Cu, Zn-SOD to furnish insights into the mechanism of the binding.

In two previous publications from this laboratory [21,28], the oxidation of xanthine catalyzed by XO and the dismutation of $O_2^{\bullet-}$ catalyzed by Cu, Zn-SOD were investigated by isothermal calorimetry. In this study, ITC and fluorescence spectroscopy were combined to study the interaction between bovine milk XO and bovine erythrocyte Cu, Zn-SOD. The results obtained indicate that XO binds to Cu, Zn-SOD with high affinity and that hydrogen bond is a major force for the binding.

2. Experimental

2.1. Materials

Bovine milk XO (Sigma Chemical Co., St. Louis, MO, USA) was centrifugated at 4 °C for 7 min at 6000 rpm. The upper layer was removed and the pellet was redissolved in 0.01 mol dm⁻³ HEPES buffer containing 0.15 mol dm⁻³ NaCl and 0.001 mol dm⁻³ EDTA (pH 7.4). Because some of FAD was also removed from XO during the process, 0.025 cm³ of 0.002 mol dm⁻³ FAD solution was added into 1 cm³ of deflavoenzyme (20 g dm⁻³ in HEPES buffer) to reconstitute the holoenzyme [31]. Then XO was dialyzed against the buffer in the dark overnight in order to remove sodium salicylate and ammonium sulfate in sample completely. The concentration of XO was determined using a molar extinction coefficient of 37,800 mol⁻¹ dm³ cm⁻¹ at 450 nm [32] and the activity of the enzyme was measured spectrophotometrically by monitoring the formation of uric acid from xanthine at 295 nm [22]. Bovine erythrocyte Cu, Zn-SOD (Sigma) was used without further purification. The concentration of Cu, Zn-SOD was determined at 258 nm using a molar extinction coefficient of 10,300 mol⁻¹ dm³ cm⁻¹ [26] and the activity of the enzyme was determined by using a pyrogallol autoxidation inhibition assay [33]. XO and Cu, Zn-SOD were both considered as a dimer in the calculations of concentrations and molar ratios. FAD and xanthine were obtained from Sigma with purity 96% and >99%, respectively. HEPES was purchased from Promega Corporation (Madison, WI, USA). All chemicals used were made in China and of analytical grade. All reagent solutions used were prepared in 0.01 mol dm⁻³ HEPES buffer containing 0.15 mol dm⁻³ NaCl (pH 7.4).

2.2. Isothermal titration calorimetry

ITC measurements were performed at 20.0, 25.0, 30.0, and 37.0 °C by using a VP-ITC titration calorimeter (MicroCal,

Northampton, MA, USA). All solutions were thoroughly degassed before use by stirring under vacuum. Before each experiment, the ITC sample cell was washed several times with HEPES buffer. The sample cell was loaded with 1.43 cm³ of Cu, Zn-SOD solution (1.30 μmol dm⁻³) and the reference cell contained doubly distilled water. Titration was carried out using a 0.25 cm³ syringe filled with XO solution, with stirring at 300 rpm. The concentrations of XO were varied between 35.0 and 52.0 μmol dm⁻³. Injections were started after baseline stability had been achieved. A titration experiment consisted of 28 consecutive injections of 0.0100 cm³ volume and 20 s duration each, with a 4 min interval between injections. Heats of dilution were determined by injecting XO into the buffer alone and the total observed heats of binding were corrected for the heat of dilution. The resulting data were fitted to a single set of identical sites model using MicroCal ORIGIN software supplied with the instrument, and the intrinsic molar enthalpy change for the binding, $\Delta_b H_m^\circ$, the binding stoichiometry, n , and the intrinsic binding constant, K_b , were thus obtained. The intrinsic molar free energy change, $\Delta_b G_m^\circ$, and the intrinsic molar entropy change, $\Delta_b S_m^\circ$, for the binding reaction were calculated by the fundamental equations of thermodynamics [6,7]:

$$\Delta_b G_m^\circ = -RT \ln K_b \quad (1)$$

$$\Delta_b S_m^\circ = \frac{\Delta_b H_m^\circ - \Delta_b G_m^\circ}{T} \quad (2)$$

The molar heat capacity change associated with the binding reaction, $\Delta_b C_{p,m}$, was thus obtained.

2.3. Intrinsic fluorescence spectroscopy

Intrinsic fluorescence spectroscopic experiments on the interaction of XO, a quencher, with Cu, Zn-SOD were carried out at 20.0, 25.0, 30.0, and 37.0 °C using a LS-55 luminescence spectrometer (Perkin-Elmer Life Sciences, Shelton, CT, USA). Because Cu, Zn-SOD contains a single tyrosine residue (Tyr 108), which is completely conserved, and no tryptophan per subunit [34], and XO contains 34 tyrosine residue and 11 tryptophan per subunit, the excitation wavelength at 280 nm was used for the intrinsic fluorescence measurements, and the emission spectra were recorded between 280 and 400 nm. The excitation and emission slits were both 8 nm, and the scan speed was 100 nm min⁻¹. 3.00 cm³ of Cu, Zn-SOD (2.78 μmol dm⁻³) was placed in a 1 cm thermostated quartz fluorescence cuvette and titrated with 0.0100 cm³ aliquots of XO (2.03 μmol dm⁻³) with continuous stirring. After each titration, the solution was mixed thoroughly and allowed to equilibrate thermally for 5 min prior to the fluorescence measurements. The fluorescence measurements of Cu, Zn-SOD and XO were carried out with optical density less than 0.1 at 258 and 295 nm, respectively, in order to avoid the inner filter effects [22]. The fluorescence data for two control systems, the buffer titrated with 0.0100 cm³ aliquots of XO and Cu, Zn-SOD titrated with

Table 1
Thermodynamic parameters for the interaction of XO with Cu, Zn-SOD at different temperatures using ITC^a

T (K)	n	$K_b \times 10^{-6}$	$\Delta_b H_m^\circ$ (kJ mol ⁻¹)	$\Delta_b G_m^\circ$ (kJ mol ⁻¹)	$\Delta_b S_m^\circ$ (J mol ⁻¹ K ⁻¹)
293.15	2.73 ± 0.06	1.20 ± 0.09	-201.1 ± 10.9	-34.0 ± 0.2	-569
298.15	3.46 ± 0.07	0.198 ± 0.011	-191.7 ± 6.6	-30.2 ± 0.1	-541
303.15	3.30 ± 0.16	0.195 ± 0.017	-167.7 ± 12.5	-30.7 ± 0.2	-452
310.15	2.73 ± 0.12	0.961 ± 0.142	-157.7 ± 9.2	-35.5 ± 0.4	-394

^a Errors shown are standard errors of the mean. Experiments were performed in 0.01 mol dm⁻³ HEPES buffer containing 0.15 mol dm⁻³ NaCl (pH 7.4).

0.0100 cm³ aliquots of buffer, were also measured under the same condition and used to correct the observed fluorescence and the dilution effects. Salt concentration dependence of the fluorescence intensity for the interaction was determined in 0.01 mol dm⁻³ HEPES buffer at NaCl concentrations in the 0–1 mol dm⁻³ range (0, 0.050, 0.15, 0.30, 0.50, and 1.0 mol dm⁻³) and at 25.0 °C. Then $\log(F_0 \Delta F / F \Delta F_{\max})$

was plotted against $\log[XO]$, and the value of K_b at each NaCl concentration was determined from the linear plot by assuming the relation that the pK_b of the complex equals the value of $[XO]$ when $\log(F_0 \Delta F / F \Delta F_{\max}) = 0$ [35,36]. Here, F_0 is the fluorescence intensity of Cu, Zn-SOD alone, F is the fluorescence intensity of Cu, Zn-SOD in the presence of a concentration of XO, and ΔF and ΔF_{\max} are the fluorescence intensity changes of Cu, Zn-SOD in the presence of a concentration of XO and saturated with XO, respectively. For the intrinsic fluorescence experiments on Cu, Zn-SOD binding to XO, 3.00 cm³ of XO (0.051 μmol dm⁻³) was titrated with 0.0100 cm³ aliquots of Cu, Zn-SOD (23.8 μmol dm⁻³) with continuous stirring. The fluorescence data for two control systems, the buffer titrated with 0.0100 cm³ aliquots of Cu, Zn-SOD and XO titrated with 0.0100 cm³ aliquots of buffer, were also measured under the same condition and used to correct the observed fluorescence and the dilution effects.

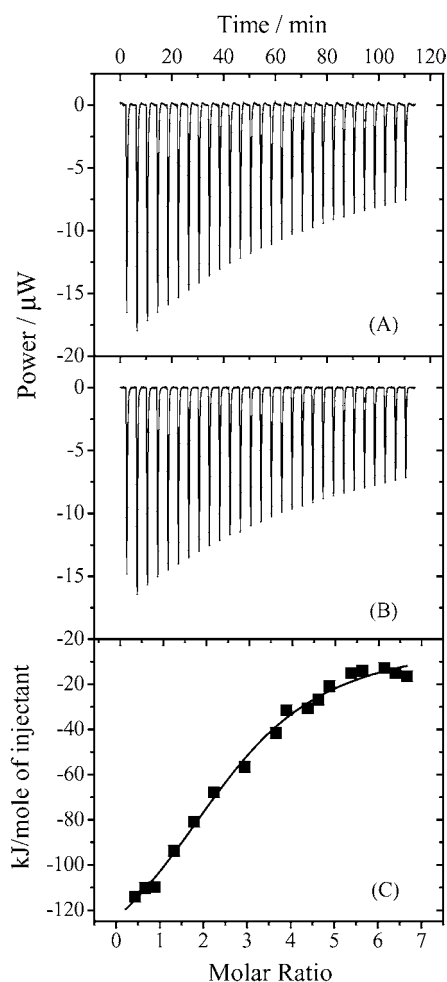


Fig. 1. ITC measurements of the binding of XO to Cu, Zn-SOD at 37.0 °C in 0.01 mol dm⁻³ HEPES buffer containing 0.15 mol dm⁻³ NaCl (pH 7.4). (A) Typical calorimetric titration of Cu, Zn-SOD (1.27 μmol dm⁻³) with XO (39.7 μmol dm⁻³). (B) The control experiment was performed in which XO solution was injected into the buffer alone. (C) Plot of the heat evolved (kJ) per mole of XO added, corrected for the heat of dilution, against the molar ratio of XO to Cu, Zn-SOD. The data (■) were fitted to a single set of identical sites model and the solid line represents the best fit.

3. Results

3.1. Thermodynamic analysis of the interaction of XO with Cu, Zn-SOD using ITC

Fig. 1A shows the ITC curve of the interaction of XO with Cu, Zn-SOD at 37.0 °C, and Fig. 1B displays a plot of the heat evolved per mole of XO added, corrected for the heat of dilution, against the molar ratio of XO to Cu, Zn-SOD. The calorimetric data were fitted to a single set of identical sites model yielding $\Delta_b H_m^\circ = -157.7 \pm 9.2$ kJ mol⁻¹, $n = 2.73 \pm 0.12$, and $K_b = (0.961 \pm 0.142) \times 10^6$. The thermodynamic parameters obtained at 20.0, 25.0, 30.0, and 37.0 °C were summarized in Table 1. As shown in Table 1, the values of n at the four temperatures examined were all around 3, suggesting a stoichiometry of one Cu, Zn-SOD subunit binding with three XO subunits.

Fig. 2 shows the temperature dependence of the intrinsic thermodynamic parameters for the binding of XO to Cu, Zn-SOD. As shown in Fig. 2, the molar heat capacity changes associated with the binding, $\Delta_b C_{p,m}$, were 2.72 kJ mol⁻¹ K⁻¹ for the plot of $\Delta_b H_m^\circ$ versus T and 3.31 kJ mol⁻¹ K⁻¹ for the plot of $\Delta_b S_m^\circ$ versus $\ln T$ with linear correlation coefficients of 0.97 and 0.98, respectively. The values of $\Delta_b C_{p,m}$ obtained from the above two plots were square with each other. The above results indicated that the molar heat capacity change of the binding was independent of temperature in the range studied. A plot of $\Delta_b H_m^\circ$ versus $T \Delta_b S_m^\circ$ for the

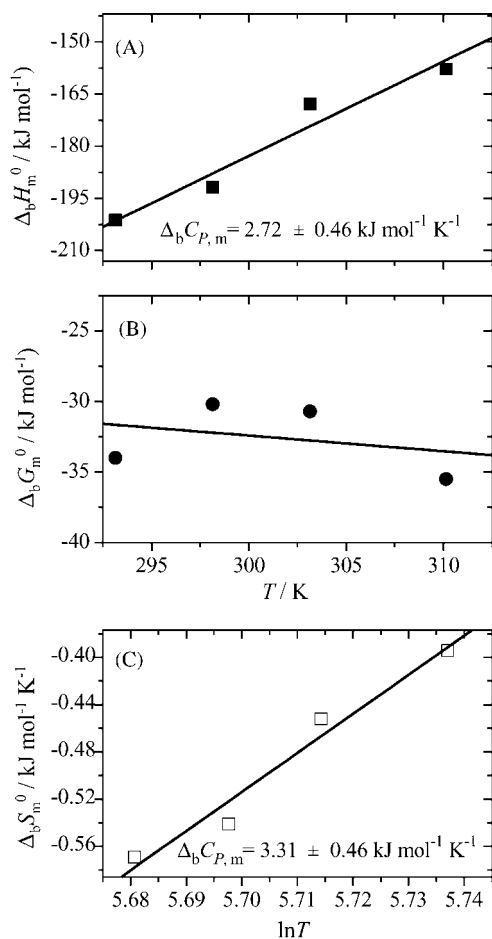


Fig. 2. Temperature dependence of the intrinsic thermodynamic parameters for the binding of XO to Cu, Zn-SOD. The intrinsic molar enthalpy change (■), the intrinsic molar free energy change (●), and the intrinsic molar entropy change (□) were determined using ITC as described in Section 2. The molar heat capacity change associated with the binding, $\Delta_b C_{p,m}$, was determined by linear regression analysis of the plot by $\Delta_b H_m^0 = \Delta_b C_{p,m}T + \Delta H^0$ (A) and $\Delta_b S_m^0 = \Delta_b C_{p,m} \ln T + \Delta S^0$ (C), respectively using the data in (A) and (C).

binding at different temperatures showed a slope of 0.96 with a linear correlation coefficient of 0.99 and an enthalpy intercept of $-38.9 \text{ kJ mol}^{-1}$, indicating strong enthalpy–entropy compensation. The ITC experiments show that XO binds to Cu, Zn-SOD with favorable enthalpy, unfavorable entropy, and high affinity.

3.2. Fluorescence quenching studies on the interaction of XO with Cu, Zn-SOD

The intrinsic tyrosine fluorescence of a protein can be exploited to detect the local changes of its environment. As shown in Fig. 3A, a regular decrease in the intrinsic fluorescence intensity of Cu, Zn-SOD tyrosine residues together with a small red shift of fluorescence emission maximum from 307.5 to 309.0 nm takes place upon increasing the concentration of XO at 25.0 °C. The quenching phenomenon was caused by the binding of XO to Cu, Zn-SOD, but not by the

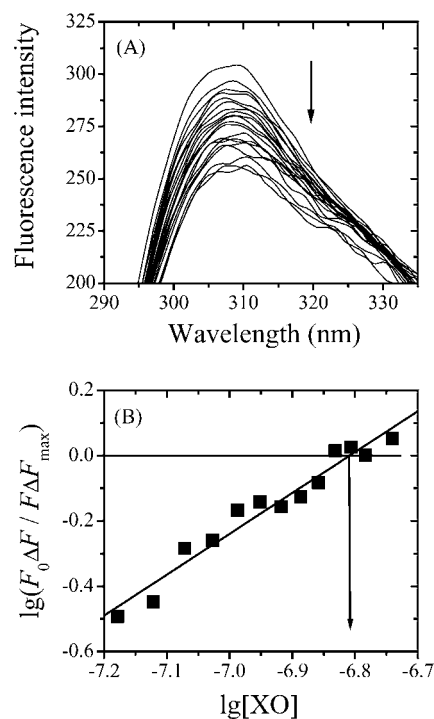


Fig. 3. Fluorescence titration measurements of the binding of XO to Cu, Zn-SOD at 25.0 °C in 0.01 mol dm⁻³ HEPES buffer containing 0.15 mol dm⁻³ NaCl (pH 7.4). (A) Intrinsic fluorescence emission spectra of Cu, Zn-SOD (2.78 μmol dm⁻³) titrated with XO (2.03 μmol dm⁻³). The arrow represents the concentration of XO increases gradually from 0 (the top) to 0.127 μmol dm⁻³ (the bottom). (B) Linear plot of $\log(F_0 \Delta F / F \Delta F_{\max})$ for the interaction of Cu, Zn-SOD with XO against $\log[\text{XO}]$. The solid squares are the experimental data and the straight line represents the best fit. The linear correlation coefficient of the fit is 0.98. Fluorescence was excited at 280 nm and the titration experiment consisted of 20 consecutive injections.

concentration decrease of Cu, Zn-SOD, which had been subtracted from the interaction. The quenching of fluorescence intensity of the protein upon the addition of XO suggests that the two tyrosine residues are either directly involved in XO binding or in the vicinity of the binding pocket. The data were fitted to $\log(F_0 \Delta F / F \Delta F_{\max})$ versus $\log[\text{XO}]$ (Fig. 3B) yielding the intrinsic binding constant for the binding at this temperature.

Salt concentration dependence of the intrinsic binding constants for the interaction of XO with Cu, Zn-SOD was determined by fluorescence spectroscopy in 0.01 mol dm⁻³ HEPES buffer at NaCl concentrations in the 0–1 mol dm⁻³ range and at 25.0 °C (Table 2). At physiologic ionic strength (0.15 mol dm⁻³ NaCl, pH 7.4), the K_b was determined to be $(6.62 \pm 1.27) \times 10^6$, and the data at 1.0 mol dm⁻³ NaCl afforded the nonionic contribution [18]. As shown in Table 2, the value of K_b was only 1.6-fold increased when NaCl concentration decreased from 1.0 mol dm⁻³ to zero, suggesting a minor role of long-range electrostatic forces for the binding [15,18,37].

As shown in Fig. 4, a regular decrease in the intrinsic fluorescence intensity of XO but no shift of fluorescence emission maximum occurs upon increasing the concentration of

Table 2

Salt concentration dependence of the intrinsic binding constants for the interaction of XO with Cu, Zn-SOD as determined by fluorescence spectroscopy at 25.0 °C^a

C_{NaCl} (mol dm ⁻³)	$K_b \times 10^{-6}$
0	7.75 ± 1.20
0.050	6.90 ± 0.71
0.15	6.62 ± 1.27
0.30	6.33 ± 2.20
0.50	5.49 ± 0.84
1.0	4.90 ± 0.60

^a Errors shown are standard errors of the mean. Experiments were performed in 0.01 mol dm⁻³ HEPES buffer containing different concentrations of NaCl (pH 7.4).

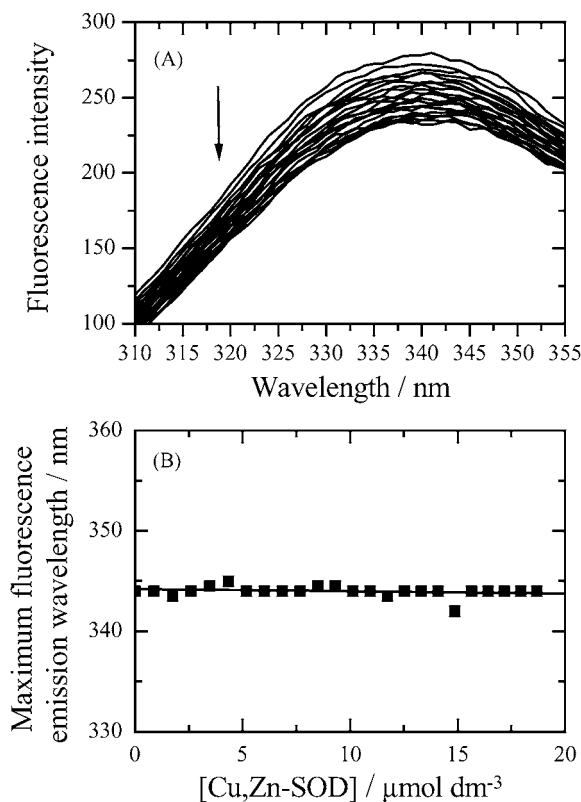


Fig. 4. Fluorescence titration measurements of the binding of Cu, Zn-SOD to XO at 25.0 °C in 0.01 mol dm⁻³ HEPES buffer containing 0.15 mol dm⁻³ NaCl (pH 7.4). (A) Intrinsic fluorescence emission spectra of XO (0.051 μmol dm⁻³) titrated with Cu, Zn-SOD (23.8 μmol dm⁻³). The arrow represents the concentration of Cu, Zn-SOD increases gradually from 0 (the top) to 1.87 μmol dm⁻³ (the bottom). (B) The intrinsic fluorescence emission maximum of XO against the concentration of Cu, Zn-SOD. Fluorescence was excited at 280 nm and the titration experiment consisted of 23 consecutive injections.

Cu, Zn-SOD. The quenching phenomenon was caused by the binding of Cu, Zn-SOD to XO, but not by the concentration decrease of XO, which had been subtracted from the interaction. The fluorescence quenching experiments show that the interaction of XO with Cu, Zn-SOD with high affinity and small structural changes.

4. Discussion

It is well known that the interactions between different proteins display certain common properties [1,9,38,39]. The negative molar heat capacity changes associated with PPIs and other non-covalent association reactions, for example, are usually attributed to the hydrophobic interaction arisen from the reduction in the number of nonpolar surface-exposed groups [1,6,16,38–41]. In contrary, the positive molar heat capacity changes associated with PPIs and other non-covalent association reactions, which are very rare [18,42,43], are commonly attributed to either hydrogen bonds or long-range electrostatic interactions arisen from the reduction in the number of polar surface-exposed groups, although other factors may contribute to $\Delta_b C_{p,m}$ [1,14,17,18,41–45]. An unexpected, large positive molar heat capacity change of the binding of XO to Cu, Zn-SOD, 3.02 kJ mol⁻¹ K⁻¹ (the average of the two values of $\Delta_b C_{p,m}$ in Fig. 2), at all temperatures examined suggests that either hydrogen bond or long-range electrostatic interaction is a major force for the binding. This is the first large positive value of $\Delta_b C_{p,m}$ reported for a PPI. To check that it is really unusual, we looked at the papers by Stites [1] and by Spolar and Record [38], which give $\Delta_b C_{p,m}$ values for a number of PPIs, and found that none of them is positive. Schreiber and Fersht [37] have pointed out that PPIs are sometimes controlled by electrostatics and hydrogen bond. Janin [46] has pointed out that long-range electrostatic forces contribute to a favorable change in entropy of interaction by maximizing the frequency of productive encounters. A small salt concentration dependence of the binding affinity measured by fluorescence spectroscopy and a large unfavorable change in entropy for the binding measured by ITC suggest that long-range electrostatic forces do not play an important role [15,18,37,46] in the binding of XO to Cu, Zn-SOD. These results indicate that hydrogen bond is a major force for the binding. The formation of hydrogen bonds between XO and Cu, Zn-SOD is attribute to their surface structures, on which there are many hydrogen bond donors or acceptors, for example, Arg 37, Asn 19, and Tyr 562 of XO [20], and Arg 127, Asp 129, and Asn 90 of Cu, Zn-SOD [27]. Because the site(s) of the interaction between the two proteins is unknown at the present time, we cannot interpret the results specifically in structural terms.

It remains unclear whether the $\Delta_b C_{p,m}$ effect is the result of dissociation of one of the interacting components, the dimer of XO or Cu, Zn-SOD. Dissociation of a dimeric protein usually results in a pronounced red shift of the intrinsic fluorescence emission maximum [8]. Only a small red shift of the intrinsic fluorescence emission maximum for Cu, Zn-SOD titrated with XO, however, occurred upon increasing the concentration of XO. Meanwhile, no shift of the intrinsic fluorescence emission maximum for XO titrated with Cu, Zn-SOD was observed during the increase of the concentration of Cu, Zn-SOD. The results showed that dissociation of one of the interacting proteins did not take place during the binding of XO to Cu, Zn-SOD. Although the results from

fluorescence spectroscopy showed that XO binds to Cu, Zn-SOD with small conformational changes, the possibility that the molar enthalpy change accompanying the conformational change in the proteins is a possible source of $\Delta_b H_m^\circ$ cannot be excluded.

Another surprising feature of the thermodynamics of the interaction of XO with Cu, Zn-SOD is the presence of entropy–enthalpy compensation, which accompanies the formation of hydrogen bonds [18,45] but not the normal hydrophobic interaction [1,6,16,38–41]. A large $\Delta_b C_{p,m}$, either negative or positive, leads to significant temperature variations in $\Delta_b H_m^\circ$ and $\Delta_b S_m^\circ$ which, nevertheless, tend to compensate to give relative smaller changes in the more functionally significant Gibbs free energy change, $\Delta_b G_m^\circ$, which is then less sensitive to temperature fluctuations [45].

Combining the results from ITC and fluorescence spectroscopy, we conclude that XO binds to Cu, Zn-SOD with high affinity and small structural changes and that hydrogen bond is a major force for the binding.

Acknowledgments

We thank Prof. Robert L. Baldwin (Stanford University School of Medicine, USA) for his critical reading of the manuscript and for his helpful suggestions. This work was supported by the National Natural Science Foundation of China (Grants 30370309 and 90408005) and the Natural Science Foundation of Hubei Province (Grant 2001abb046).

References

- [1] W.E. Stites, *Chem. Rev.* 97 (1997) 1233.
- [2] G. Schreiber, *Curr. Opin. Struct. Biol.* 12 (2002) 41.
- [3] H. Gohlke, C. Kie, D.A. Case, *J. Mol. Biol.* 330 (2003) 891.
- [4] A.V. Veselovsky, Y.D. Ivanov, A.S. Ivanov, A.I. Archakov, P. Lewi, P. Janssen, *J. Mol. Recognit.* 15 (2002) 405.
- [5] S. Leavitt, E. Freire, *Curr. Opin. Struct. Biol.* 11 (2001) 560.
- [6] Y. Liang, J. Li, J. Chen, C.C. Wang, *Eur. J. Biochem.* 268 (2001) 4183.
- [7] Y. Liang, F. Du, B.R. Zhou, H. Zhou, G.L. Zou, C.X. Wang, S.S. Qu, *Eur. J. Biochem.* 269 (2002) 2851.
- [8] Y. Liang, F. Du, S. Sanglier, B.R. Zhou, Y. Xia, A. Van Dorsselaer, C. Maechling, M.C. Kilhoffer, J. Haiech, *J. Biol. Chem.* 278 (2003) 30098.
- [9] P.C. Weber, F.R. Salemme, *Curr. Opin. Struct. Biol.* 13 (2003) 115.
- [10] M.J. Cliff, J.E. Ladbury, *J. Mol. Recognit.* 16 (2003) 383.
- [11] D.G. Myszka, R.W. Sweet, P. Hensley, M. Brigham-Burke, P.D. Kwong, W.A. Hendrickson, R. Wyatt, J. Sodroski, M.L. Doyle, *Proc. Natl. Acad. Sci. U.S.A.* 97 (2000) 9026.
- [12] J. Dong, C.A. Peters-Libeau, K.H. Weisgraber, B.W. Segelke, B. Rupp, I. Capila, M.J. Hernaiz, L.A. LeBrun, R.J. Linhardt, *Biochemistry* 40 (2001) 2826.
- [13] M.J. Hernaiz, L.A. LeBrun, Y. Wu, J.W. Sen, R.J. Linhardt, N.H.H. Heegaard, *Eur. J. Biochem.* 269 (2002) 2860.
- [14] H.I. Jung, A. Cooper, R.N. Perham, *Biochemistry* 41 (2002) 10446.
- [15] P.K. Nielsen, B.C. Bønsager, C.R. Berland, B.W. Sigurskjold, B. Svensson, *Biochemistry* 42 (2003) 1478.
- [16] Z. Lin, F.P. Schwarz, E. Eisenstein, *J. Biol. Chem.* 270 (1995) 1011.
- [17] K. Aoke, H. Taguchi, Y. Shindo, M. Yoshida, K. Ogasahara, K. Yutani, N. Tanaka, *J. Biol. Chem.* 272 (1997) 32158.
- [18] R.E. Hileman, R.N. Jennings, R.J. Linhardt, *Biochemistry* 37 (1998) 15231.
- [19] V. Massey, L.M. Schopfer, T. Nishino, T. Nishino, *J. Biol. Chem.* 264 (1989) 10567.
- [20] C. Enroth, B.T. Eger, K. Okamoto, T. Nishino, E.F. Pai, *Proc. Natl. Acad. Sci. U.S.A.* 97 (2000) 10723.
- [21] Y. Liang, C.X. Wang, S.S. Qu, Y.X. Wu, D.H. Li, G.L. Zou, *Thermochim. Acta* 322 (1998) 1.
- [22] A.K. Sau, S. Mitra, *Biochim. Biophys. Acta* 1481 (2000) 273.
- [23] T. Oda, T. Akaike, T. Hamamoto, F. Suzuki, T. Hirano, H. Maeda, *Science* 244 (1989) 974.
- [24] J.M. Matés, C. Pérez-Gómez, I.N. de Castro, *Clin. Biochem.* 32 (1999) 595.
- [25] J.A. Tainer, E.D. Getzoff, K.M. Beem, J.S. Richardson, D.C. Richardson, *J. Mol. Biol.* 160 (1982) 181.
- [26] J.M. McCord, I. Fridovich, *J. Biol. Chem.* 244 (1969) 6049.
- [27] J.A. Tainer, E.D. Getzoff, J.S. Richardson, D.C. Richardson, *Nature* 306 (1983) 284.
- [28] Y. Liang, S.S. Qu, C.X. Wang, G.L. Zou, Y.X. Wu, D.H. Li, *Chem. Eng. Sci.* 55 (2000) 6071.
- [29] G.D. Mao, P.D. Thomas, G.D. Lopaschuk, M.J. Poznansky, *J. Biol. Chem.* 268 (1993) 416.
- [30] E. Kosenko, N. Venediktova, Y. Kaminsky, C. Montoliu, V. Felipo, *Brain Res.* 981 (2003) 193.
- [31] H. Komai, V. Massey, G. Palmer, *J. Biol. Chem.* 244 (1969) 1692.
- [32] V. Massey, P.E. Brumby, H. Komai, G. Palmer, *J. Biol. Chem.* 244 (1969) 1682.
- [33] S. Marklund, G. Marklund, *Eur. J. Biochem.* 47 (1974) 469.
- [34] S.T. Ferreira, L. Stella, E. Gratton, *Biophys. J.* 66 (1994) 1185.
- [35] D.M. Chipman, V. Grisaro, N. Sharon, *J. Biol. Chem.* 242 (1967) 4388.
- [36] S.S. Hegde, T.K. Dam, C.F. Brewer, J.S. Blanchard, *Biochemistry* 41 (2002) 7519.
- [37] G. Schreiber, A.R. Fersht, *Nature Struct. Biol.* 3 (1996) 427.
- [38] R.S. Spolar, M.T. Record Jr., *Science* 263 (1994) 777.
- [39] R.S. Spolar, J.-H. Ha, M.T. Record Jr., *Proc. Natl. Acad. Sci. U.S.A.* 86 (1989) 8382.
- [40] K.P. Murphy, P.L. Privalov, S.J. Gill, *Science* 247 (1990) 559.
- [41] V.V. Loladze, D.N. Ermolenko, G.I. Makhataдзе, *Protein Sci.* 10 (2001) 1343.
- [42] A. Niedzwiecka, J. Stepinski, E. Darzynkiewicz, N. Sonenberg, R. Stolarski, *Biochemistry* 41 (2002) 12140.
- [43] L. Neumann, R. Abele, R. Tampé, *J. Mol. Biol.* 324 (2002) 965.
- [44] Y. Li, M. Urrutia, S.J. Smith-Gill, R.A. Mariuzza, *Biochemistry* 42 (2003) 11.
- [45] A. Cooper, *Biophys. Chem.* 85 (2000) 25.
- [46] J. Janin, *Proteins Struct. Funct. Genet.* 28 (1997) 153.